PERGAMON

International Journal of Heat and Mass Transfer 42 (1999) 2543–2556

International Journal of HEAT and MASS TRANSFER

Process intensification: heat and mass transfer characteristics of liquid films on rotating discs

A. Aoune, C. Ramshaw*

Centre for Process Intensification and Innovation, Department of Chemical and Process Engineering, University of Newcastle upon Tyne, Newcastle NE1 7RU, U.K.

Received 9 February 1998; in final form 8 October 1998

Abstract

A novel high intensity heat pump [5] is comprised of a series of discs housed within a hermetically sealed rotating envelope. Each disc is irrigated with a thin film of working fluid as it performs one of the functions (e.g. absorption, evaporation, etc.) within the heat pump cycle. This paper examines the theoretical and experimental performance of these thin films when performing heat and mass transfer to the disc and the surrounding gas, respectively. It is found that very high transfer coefficients can be achieved at modest disc speeds with water-like liquids. However, at higher viscosities, the heat transfer performance is significantly reduced as might be expected. The experimental transfer coefficients are much higher than those predicted by a simple analysis based upon the film or penetration theory. This is attributed to mixing within the film.

Nomenclature

D diffusivity [$m^2\ s^{-1}$]
F Fourier number
h heat transfer coefficient [$W\ m^{-2}\ K^{-1}$]
k thermal conductivity [$W\ m^{-1}\ K^{-1}$]
M mass flowrate [$kg\ s^{-1}$]
r radius [m]
r_0 peripheral radius [m]
r_i radius at feed point [m]
t time [s]
T temperature [K]
u velocity [$m\ s^{-1}$]
y co-ordinate $\perp r$ disc surface [m].

Greek symbols
δ film thickness [m]
ρ liquid density [$kg\ m^{-3}$]
τ shear stress [$N\ m^{-2}$]
ω angular velocity [s^{-1}].

* Corresponding author.

1. Introduction

The principal targets of the process intensification (PI) strategy are to reduce the capital cost of process systems, improve their intrinsic safety and minimise their environmental impact. These desirable objectives may be achieved provided the size of individual plant items can be dramatically reduced (say by 1000 fold in volume) and where appropriate, multi-functional processing modules can be devised. Thus, hazardous process inventories, expensive pipe runs/foundations/support structure, etc., can be largely eliminated. Ideally the PI strategy should be applied across the whole plant spectrum, perhaps with particular emphasis on the reactor which is the heart of most processes.

In this context the operating characteristics of spinning discs are of considerable interest when performing gas/liquid/solid contacting operations. This is due to the elevated acceleration environment which can be created on the disc which allows the generation of thin, highly sheared films when liquid drains outwards while in contact with the disc surface. Rotation of the heat/mass transfer surface has already been recognised [1, 2] as an intensification technique and has the following potential

0017–9310/99/$ - see front matter
PII: S0017-9310(98)00336-6

advantages over other active methods for enhancing performance, such as stirring/scraping/vibrating/pulsing:

(a) Variations in the rotational speed offers an extra degree-of-freedom in equipment design.
(b) The enhanced acceleration, coupled if necessary with a suitably contrived surface structure, enhances the film processes.
(c) The disc is resistant to fouling or plugging and can handle slurries or viscous fluids.
(d) Very short contact times can be achieved which may significantly extend the reactors performance/temperature 'envelope'.

In a seminal study of the flow of liquid films down a smooth inclined plane, Brauner and Maron [3] showed that they were unstable and moreover that most of the mass transfer was associated with the fluid circulation which accompanied each ripple. The unstable nature of the liquid flow was confirmed by Woods [4] who examined the behaviour of an ink film on a 0.3 m rotating glass disc as it emanated from a central axisymmetric distributor (Figs 1–3). It can be clearly seen that the initially uniform film breaks down into well-defined spiral ripples, which then break down further into a confused assembly of wavelets.

The work described below was initiated in order to evaluate the disc/film heat transfer performance and the film/gas mass transfer performance, with a view to providing design data for an intensified absorption heat pump [5] which involves a novel design concept. The working cycle of the single effect version of this machine is outlined in Fig. 4. All the key cycle functions involve heat or mass transfer with a gas/liquid system. As noted above, the overall operation should be beneficially influenced when performed in an enhanced acceleration field. The machine which ultimately emerged from the early development programme is shown schematically in Fig. 5. It consists of an hermetically sealed rotating module comprising a series of discs which perform the heat and mass transfer functions required within the absorption operating cycle. While the results obtained are particularly relevant to the wider issues raised by the intensification strategy mentioned above, the immediate target of the work described below was to achieve a major enhancement of the performance of the absorption stage of the cycle, as this was the main factor limiting the cycle efficiency.

2. Experimental arrangement

The apparatus consisted of a 2.5 cm thick 50 cm diameter brass sub-disc assembly which could be rotated at up to 900 rpm (Fig. 6). This provided a platform for the support and rotation of various brass top disc options having alternative surface profiles, though only the

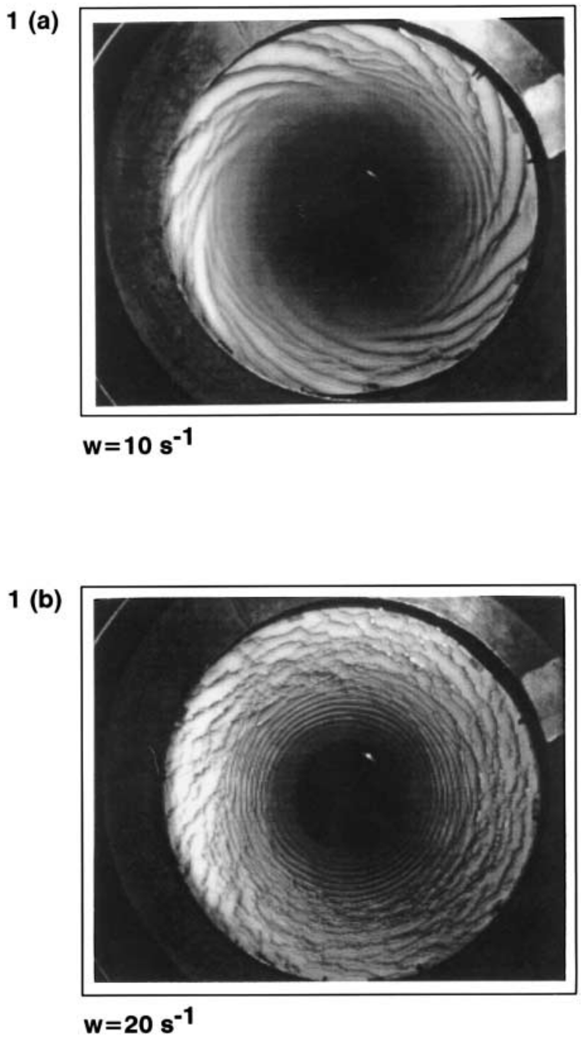

Fig. 1. Variation of wavefront across disc: $M = 1.9 \times 10^{-2}$ kg s^{-1}.

results from the smooth disc will be reported here. Thermocouples were located in the top disc in various angular and radial positions both 9 and 1 mm from the surface of the top disc. The analogue thermocouple signals were lead via the sub-disc assembly to a Datascan digitiser at the base of the drive shaft. They were then sent to a data logger via a slip ring. The signals were digitised because it was realised that an unacceptable degree of corruption was being caused by the frictional heating in the slip ring assembly.

Disc heating was provided by three pairs of radiant heating elements located 40 mm below the sub-disc. Each pair gave a maximum heat output of 2.75 kW. Brass was used for the discs in a vain attempt to ensure that the operating temperature was uniform throughout the disc. In view of this problem, the local temperature gradient

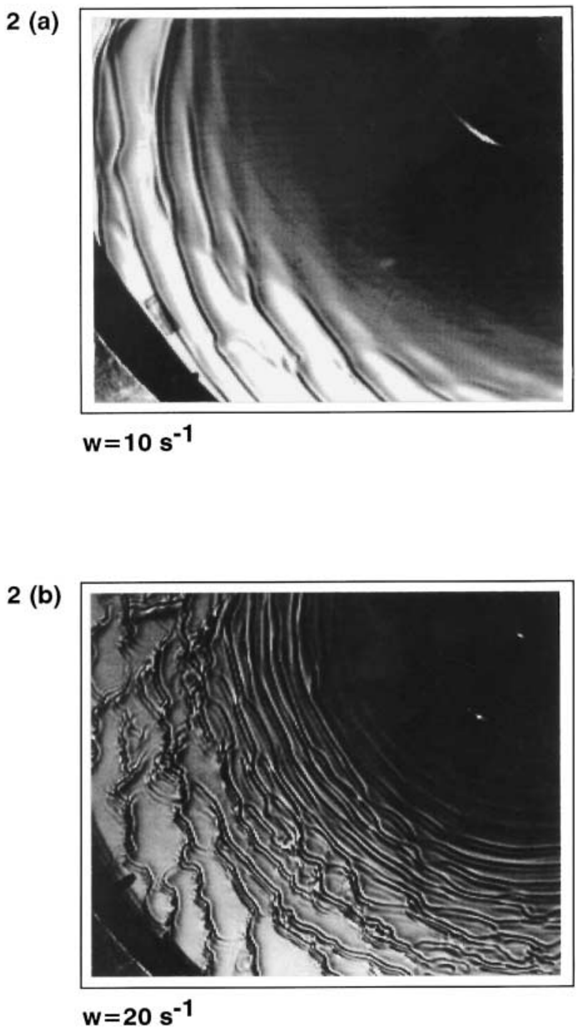

Fig. 2. Local variation of wavefronts: $M = 1.9 \times 10^{-2}$ kg s^{-1}.

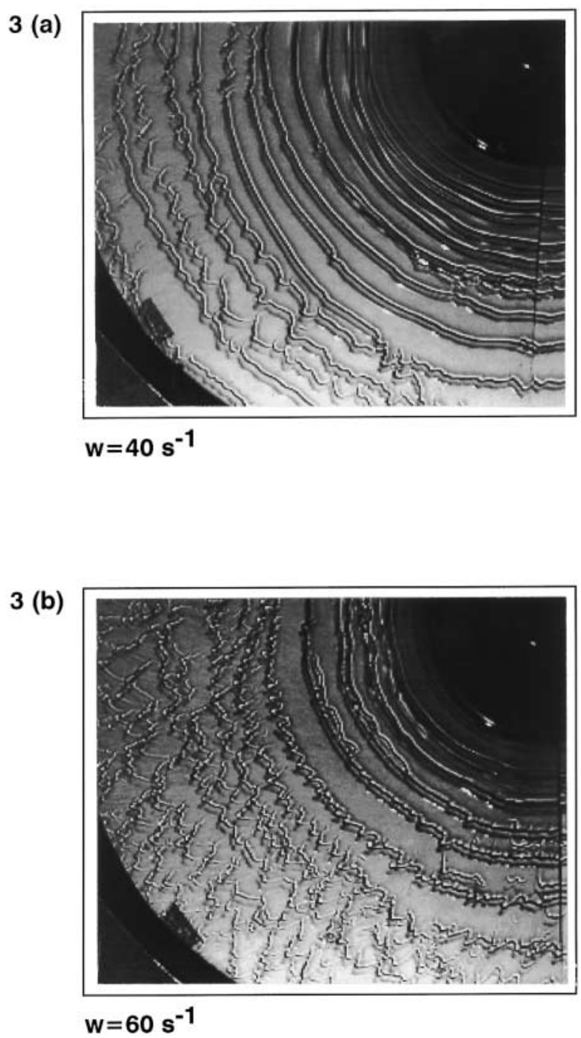

Fig. 3. Local variation of wavefronts: $M = 1.3 \times 10^{-2}$ kg s^{-1}.

normal to the disc surface was obtained by smoothing the temperature output from two sets of seven thermocouples embedded 9 and 1 mm from the disc surface. The local disc surface temperature was then calculated by extrapolating from that at 1 mm depth. The liquid film temperature was measured with a thermistor which had previously been calibrated using a high precision platinum thermometer ($\pm 10^{-3}$°C). The accuracy of the thermistor and thermocouples was $\pm 10^{-2}$°C, ± 0.1°C, respectively. Various smoothed liquid film and disc temperature profiles for a typical run are shown in Fig. 7. Bearing in mind that the disc surface temperature would typically reach 40°C during the heat transfer experiments, a significant proportion of the heat loss from the disc would be due to evaporation from the liquid film, if the disc surface were fully exposed and able to circulate the relatively dry laboratory atmosphere. Since the purpose of the heat transfer study was to examine the transmission of sensible heat across the liquid film, it was necessary to reduce the vaporisation heat load as far as possible. This was done by shrouding the disc and its cylindrical enclosure with aluminium foil and insulating material so that the disc rotated in an atmosphere which was fully saturated at the operating temperature.

Mass transfer experiments were performed by first stripping oxygen from the working fluid to a concentration of about 0.2 ppm. The liquid was then supplied to the disc which was exposed to air and liquid samples were abstracted from the film at various disc radii using an angled offtake pipe. After some manipulation, requiring considerable dexterity, a bubble-free liquid sample could be obtained for O_2 appraisal by the Orbisphere digital analyser at the necessary flowrate (>50 cm^3 min^{-1}). The dissolved oxygen concentration in equi-

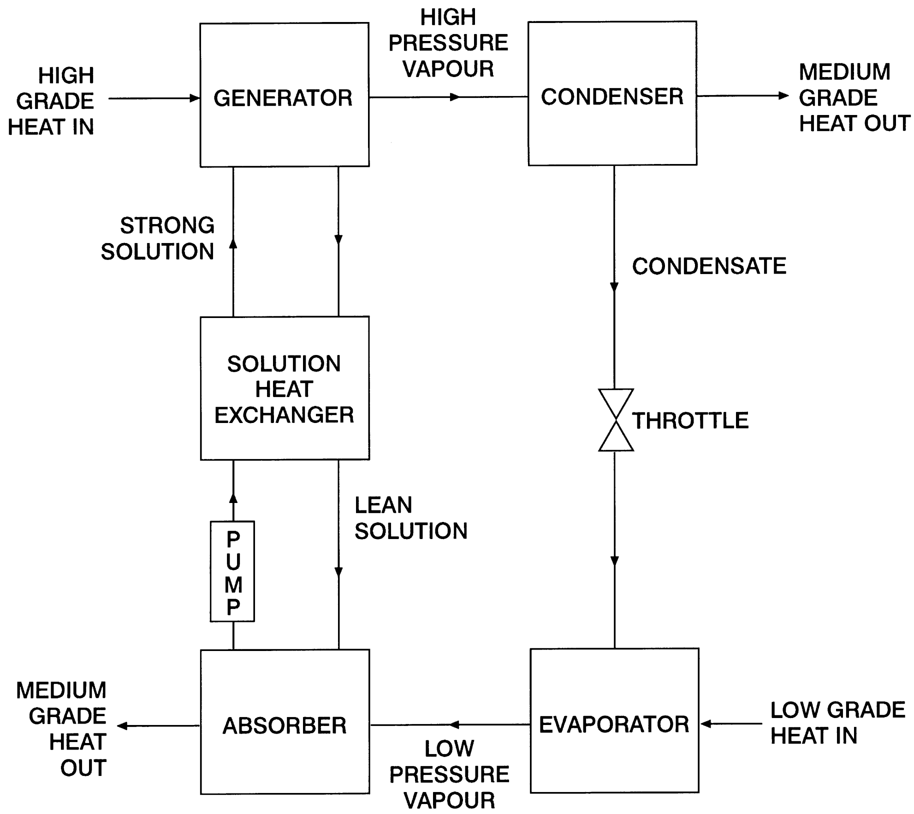

Fig. 4.The single effect absorption heat pump cycle.

librium with air at 20°C is about 9 ppm and the liquid film concentration approached this value asymptotically as the disc edge was approached, making the derived mass transfer coefficients progressively less accurate. Therefore, all mass transfer runs with a peripheral film concentration exceeding 95% of the equilibrium value, were ignored. The fluids used for both the heat and mass transfer tests were:

(a) Water.
(b) 40% water/60% propylene glycol ($\mu = 0.01$ Ns m^{-2}).

3. Analysis of liquid films on rotating discs

As already pointed out, the fluid dynamic environment existing within a film as it moves outwards over the surface of a rotating disc, is very complex. Nusselt [6] faced an analogous situation when he tackled the heat transfer problem presented by films of condensate draining under the influence of terrestrial gravitation. He ignored flow instabilities and assumed that steady state conditions existed throughout the flow field.

Since the ripples are expected to enhance the heat and mass transfer rates, any predictions based on a Nusselt-style analysis should be conservative. His approach should, however, be more realistic in predicting the performance with higher viscosity liquids, because then viscous damping of incipient ripples is more effective and a smoother film is generated.

In order to calculate the disc/film heat transfer and the gas/film mass transfer we need values for both the local film thickness and the liquid residence time. These can be calculated as follows, with reference to Fig. 8. The simple analysis is based on the following assumptions:

(a) There is no shear stress exerted by the gas on the liquid.
(b) The liquid is Newtonian.
(c) The disc axis is vertical.
(d) Liquid is introduced to the disc surface in an axi-symmetric manner.
(e) Liquid instantaneously reaches the local disc velocity (i.e. no angular slip).
(f) The film moves radially over the disc surface (i.e. the Coriolis acceleration is neglected).
(g) No heat crosses the gas/liquid interface.
(h) Radial temperature, velocity and concentration gradients are small compared with those perpendicular to the disc.

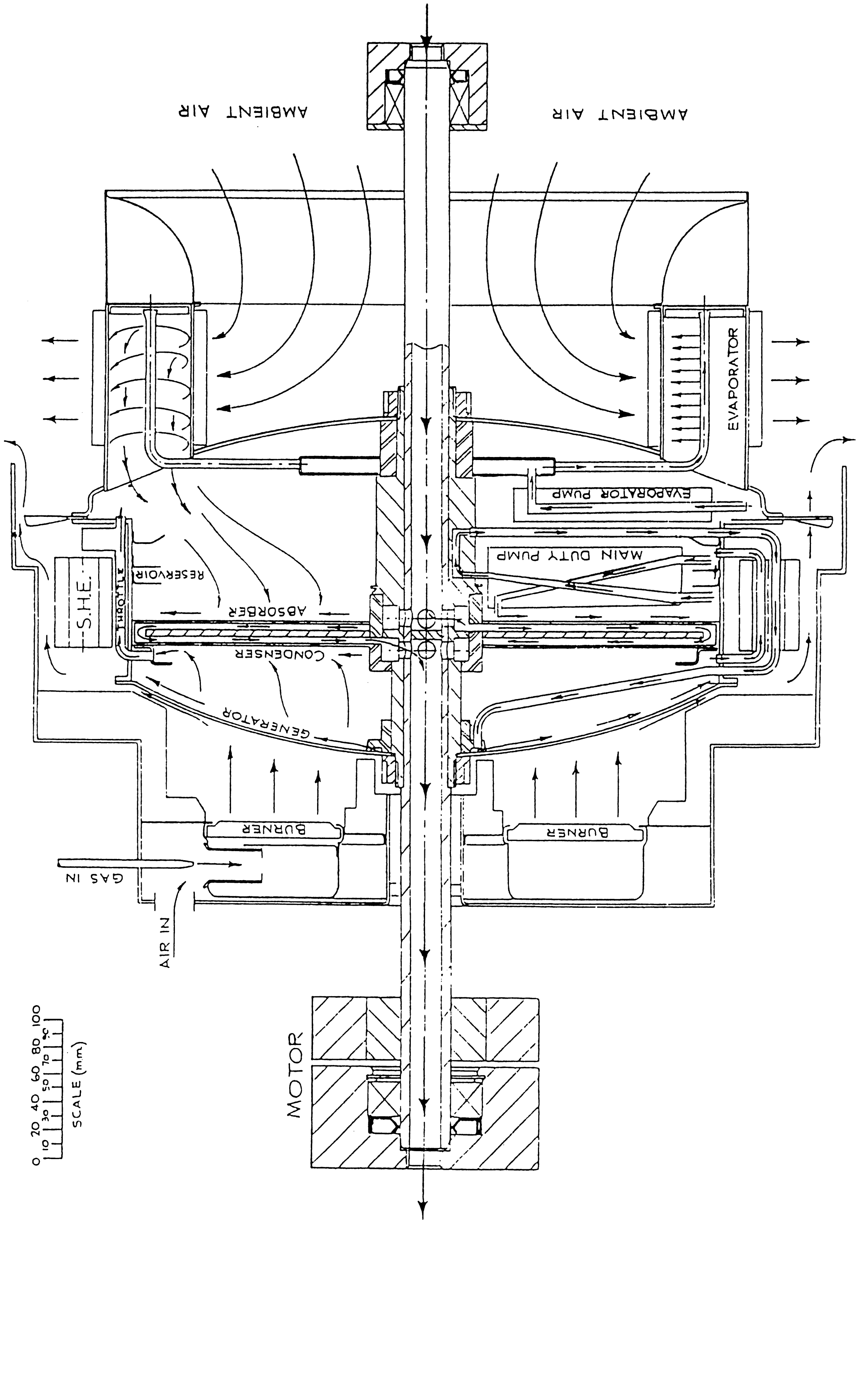

Fig. 5. General layout—rotex first prototype.

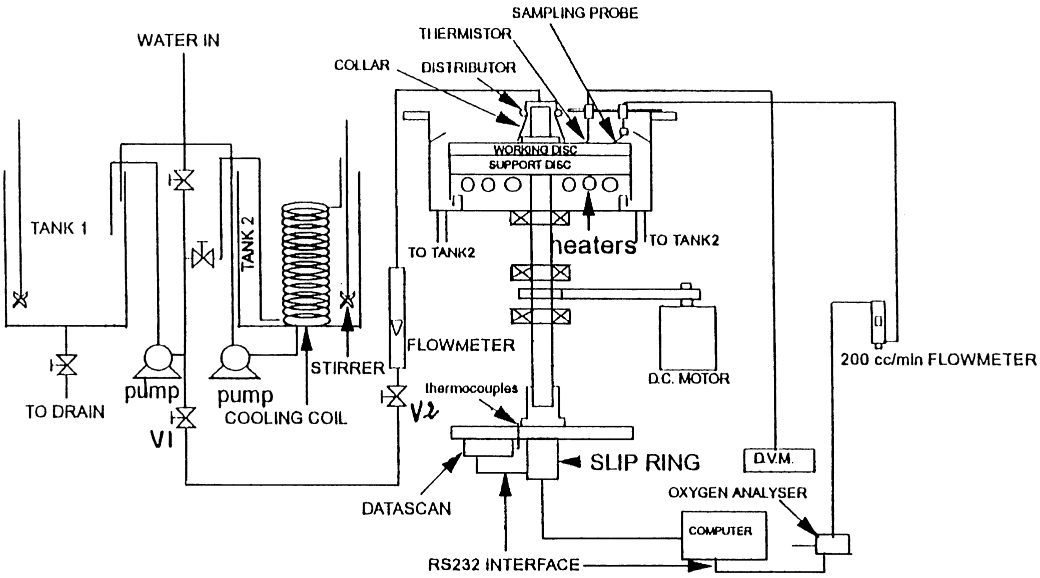

Fig. 6. Heat and mass transfer test rig.

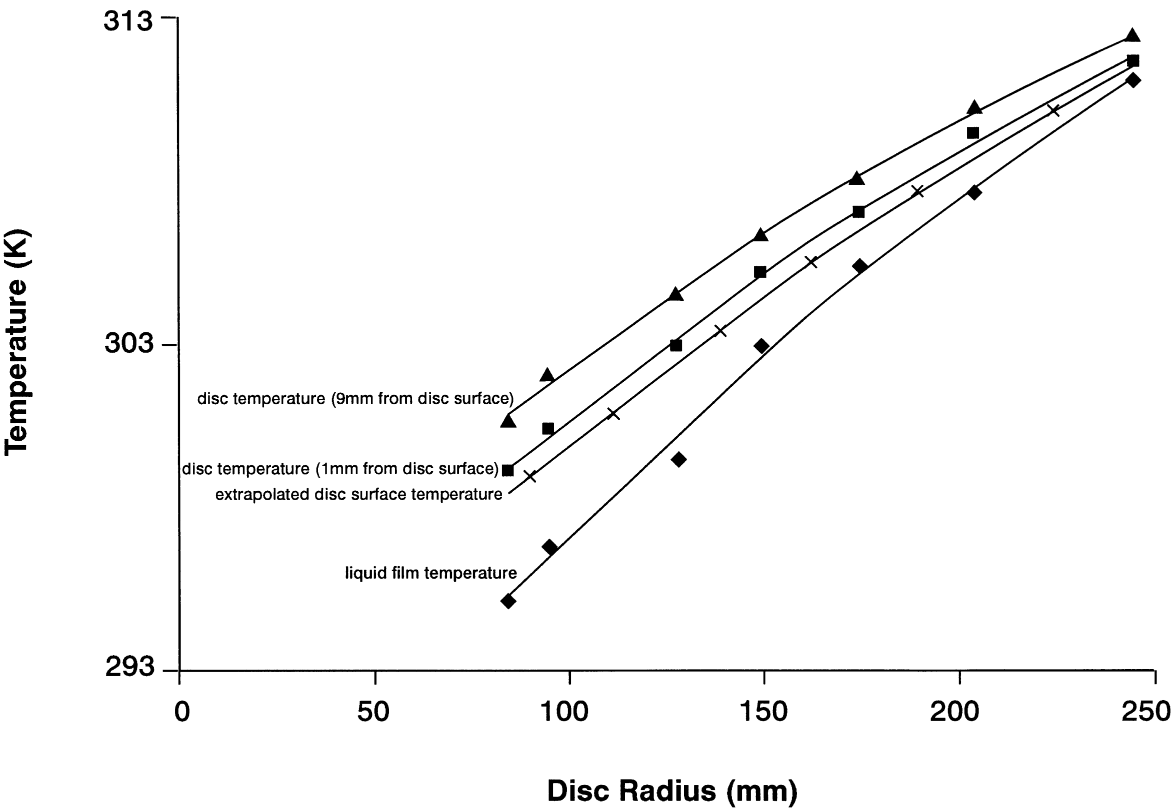

Fig. 7. Typical example of temperature distribution profiles.

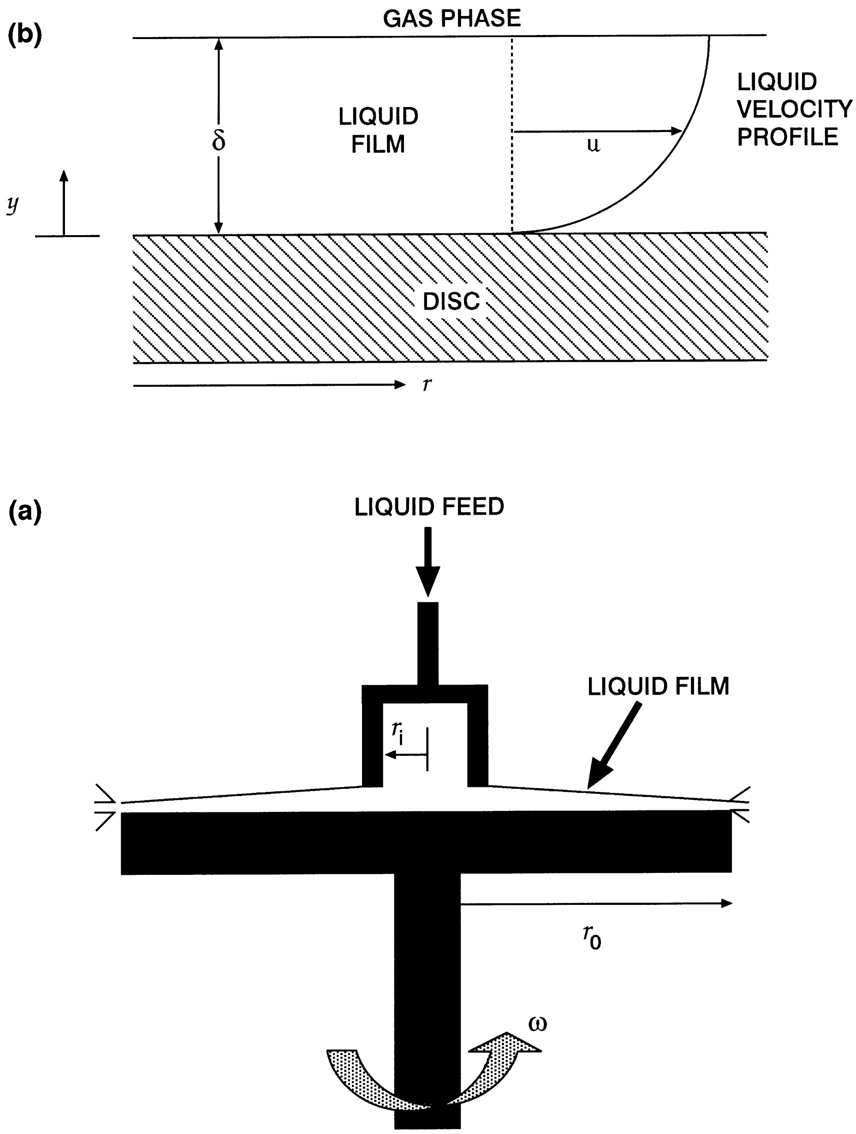

Fig. 8. Schematic arrangement of (a) the disc; (b) the liquid film.

Since the shear stress at the gas–liquid interface is zero, the body force exerted on the film between $y = y$ and $y = \delta$ is equal to the shear force at $y = y$, i.e. $t \cdot 2\pi r\,\mathrm{d}r = \omega^2 r\rho(\delta - y) \cdot 2\pi r\,\mathrm{d}r$ where the shear stress at y is given by τ.

Thus,

$$\tau = \mu \frac{\mathrm{d}u}{\mathrm{d}y} = \omega^2 r\rho(\delta - y). \tag{1}$$

Noting that $u = 0$ when $y = 0$ and invoking the assumption above that radial velocity gradients are small compared with those within the film at a given radius, we can integrate (1) to give

$$u = \frac{\omega^2 r}{\mu} \cdot \rho \left(\delta y - \frac{y^2}{2}\right).$$

Hence,

$$u_{\mathrm{MAX}} = \frac{\omega^2 r}{2\mu} \rho \delta^2 \tag{2}$$

for $y = \delta$ and

$$u_{AV} = \frac{1}{\delta}\int_{y=0}^{y=\delta} u\,dy = \frac{\omega^2 r\rho\delta^2}{3\mu}. \tag{3}$$

This is the value obtained by Nusselt for vertical drainage if $\omega^2 r$ is set equal to the terrestrial acceleration g. In order to calculate the liquid residence time and film thickness at various radial positions we note that the liquid mass flowrate is given by

$$M = \rho u_{AV}\cdot 2\pi r\delta = \frac{2\pi r^2\omega^2\rho^2}{3\mu}\delta^3. \quad \text{(from 2)}$$

Hence,

$$\delta = \left(\frac{3\mu M}{2\pi r^2\omega^2\rho^2}\right)^{1/3}. \tag{4}$$

Inserting (4) in (3) gives

$$u_{AV} = \frac{\rho\omega^2 r}{3\mu}\cdot\left(\frac{3\mu M}{2\pi r^2\omega^2\rho^2}\right)^{2/3} = \left(\frac{M^2\omega^2}{12\pi^2\rho\mu}\right)^{1/3} r^{-1/3}. \tag{5}$$

Hence, the average time needed for the liquid to travel from a feed radius r_i to the peripheral radius r_0 is $t_{AV} = \int_{r_i}^{r_0}(dr/u_{AV})$ and using (5) we have

$$t_{AV} = \frac{3}{4}\cdot\left(\frac{12\pi^2\rho\mu}{M^2\omega^2}\right)^{1/3}(r_0^{4/3} - r_i^{4/3}). \tag{6}$$

Noting from equations (2) and (3), that the velocity of the liquid layer at the gas/liquid surface (u_{MAX}) is 50% greater than the mean value u_{AV}, the corresponding minimum liquid residence time at the liquid film surface is $\frac{2}{3}t_{AV}$.

The operating conditions: $M = 6\times10^{-2}$ kg s^{-1}, $\omega = 60$ s^{-1}, $r_0 = 0.25$ m, $\mu = 10^{-3}$ Ns m^{-2}, $\rho = 10^3$ kg m^{-3} are reasonably representative of those covered in the experiments. In this case the mid-radial water film thickness predicted by equation (4) is about 80 μ, the average film residence time is 0.22 s and the film surface residence time is 0.14 s.

For water the thermal diffusivity is 1.4×10^{-7} m^2 s^{-1} and the diffusivity of oxygen in water is about 1.8×10^{-9} m^2 s^{-1}. On the ideal assumption that the film temperature and concentration profiles are dictated by unsteady one-dimensional diffusion into a slab of material, the general solutions provided by Carslaw and Jaeger [7] can be used to assess the extent to which the profiles 'penetrate' the film. In Fig. 9 the parameter is the Fourier number (F) which, as can be seen, must be >1 in order to ensure effective penetration and therefore, complete involvement of the film in the transfer process. For the liquid surface conditions given above, F for oxygen mass transfer is $(Dt/\delta^2) = 0.04$ and is 3.1 for heat transfer (noting that $y = \delta$ corresponds to $x/l = 1$ in Fig. 9). Thus, the entire film is involved in a quasi-steady state heat transfer operation, while only a surface layer takes part in the unsteady state mass transfer process. These two situations have given rise to alternative interpretations of the heat and mass transfer rates, e.g. the Whitman [8] film theory and the Higbie [9] penetration theory.

The Nusselt treatment of condensing heat transfer was based on the assumption that latent heat was conducted from the gas–liquid interface at a temperature T_s to the cooled wall at a temperature T_w. This gives rise to a heat transfer coefficient $h = (k/\delta)$. However, in the present case it is assumed that there is no heat flux across the gas–liquid interface as the liquid film approaches the wall temperature. With the comparatively high Fourier numbers noted above for heat transfer, it is reasonable from Fig. 9 to assume that the temperature distribution is approximately parabolic. On this basis the average mixed film temperature which was measured during the experiments is given by

$$T_{AV} = \frac{\int_0^\delta uT\,dy}{u_{AV}\delta}.$$

Noting that the parabolic temperature distribution which satisfies the conditions $T = T_w$ at $y = 0$, $T = T_s$ at $y = \delta$, $(dT/dy) = 0$ at $y = \delta$, is

$$T = T_w - \frac{2(T_w - T_s)}{\delta}y + \frac{(T_w - T_s)}{\delta^2}y^2$$

then it can be shown that $T_{AV} = T_w + \frac{3}{5}(T_s - T_w)$. Thus, the local film coefficient predicted on the basis of the simple Nusselt theory is

$$h = \frac{\text{heat flux}}{T_w - T_{AV}} = \frac{k}{\delta}\frac{(T_w - T_s)}{(T_w - T_{AV})} = \frac{5}{3}k\left(\frac{2\pi\omega^2\rho^2}{3\mu m}\right)^{1/3} r^{2/3}. \tag{7}$$

Values of h based on equation (7) are plotted for comparison with the experimental data in Figs 10 and 11.

On the other hand with respect to mass transfer, the Higbie penetration theory for the same film shows that the average mass transfer coefficient for a surface element which has been exposed for a time t is $h_D = 2(D/\pi t)^{1/2}$ and the point value is $h_D = (D/\pi t)^{1/2}$.

4. Results and discussion

Heat and mass transfer results are presented for a smooth 0.5 m diameter disc for a limited range of flowrate and rotational speeds in Figs 10–17. Since the absorption stage of the rotary absorption heat pump [5] was critical in determining the overall heat pumping performance of the machine, the operating conditions chosen for the disc experiments broadly represented those encountered by the machine's absorber disc. In particular, the rotational speed and liquid flows were limited by the need to restrict parasitic power loss, though it was expected that higher values would be conducive to a higher performance. Despite this the achieved performance was very high and

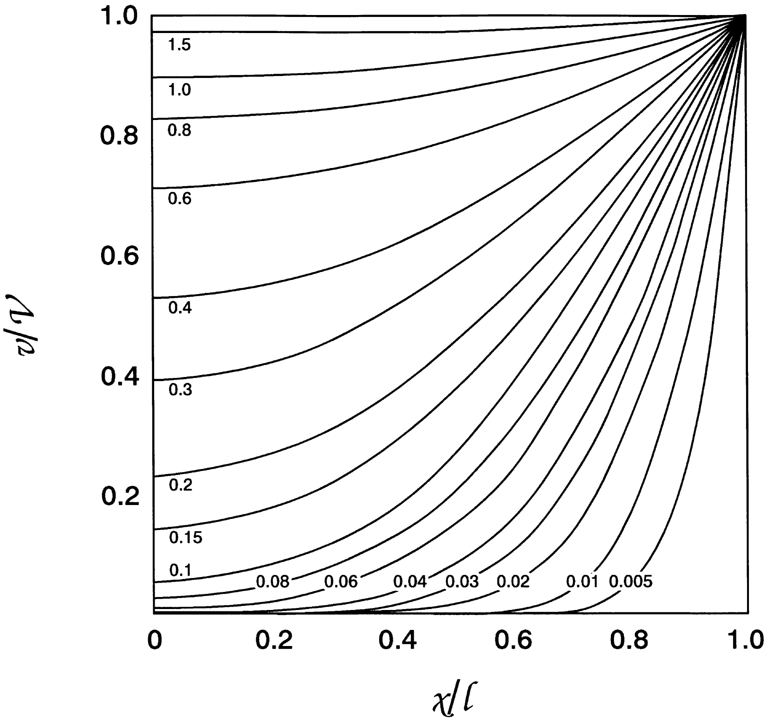

Fig. 9. Temperature distribution at various times in the slab $-l < \chi < l$ with zero initial temperature and surface temperature V. The numbers on the curves are the values of Dt/l^2.

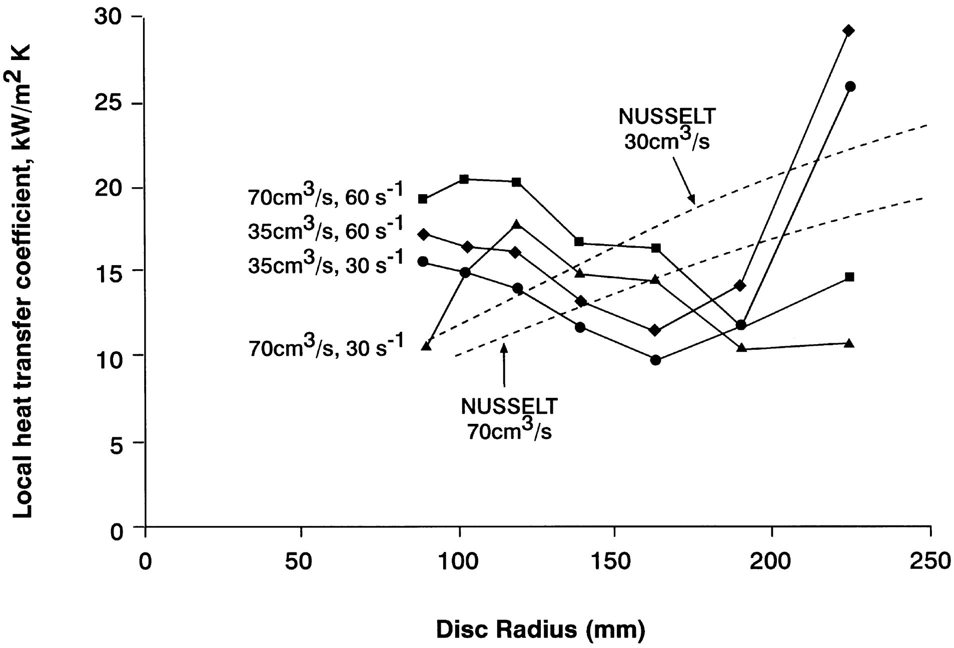

Fig. 10. Comparison of local heat transfer coefficient on smooth disc for two rotational speeds and flowrates working fluid: water.

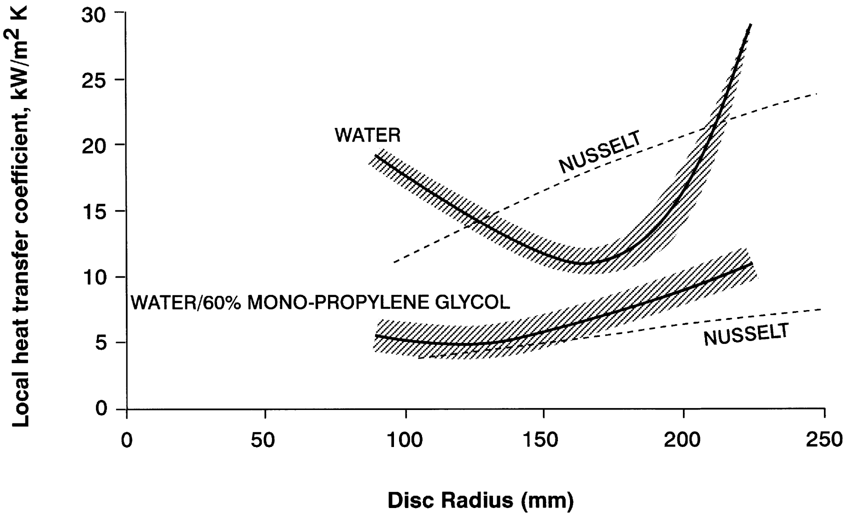

Fig. 11. Local liquid film heat transfer coefficient on smooth disc (water): 35 $cm^3 s^{-1}$, 60 s^{-1}.

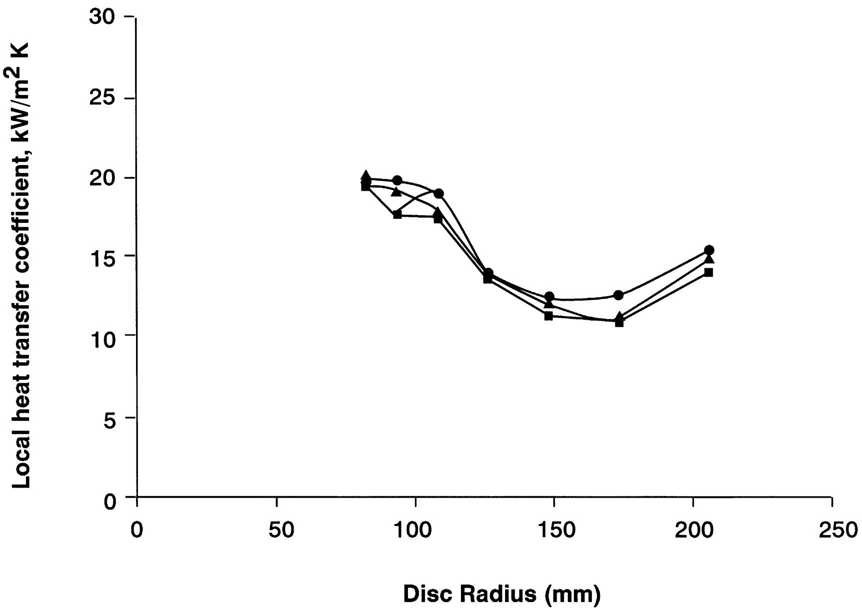

Fig. 12. Local liquid film heat transfer coefficient on smooth disc (water): 52.5 $cm^3 s^{-1}$, 60 s^{-1}.

may be expected to be even better with alternative disc geometries. The experimental reproducibility is acceptable, as shown by the groups of repeat runs shown in Figs 11–13. With water, not only were the heat transfer coefficients high at the periphery, there was also a well-defined trend for them to be raised at the inner radial positions. The latter characteristic was not expected as the simple Nusselt analysis suggested that the inner film would be comparatively thick. The anomalous behaviour is attributed to the extra film disturbance involved in bringing the feed liquid to the local disc angular velocity. It was expected that the Nusselt predictions for water would be very conservative in view of their neglect of wave enhancement. Figures 10 and 11 suggest that this was not the case, even after allowing for the inner film disturbance noted above. As the explanation for this behaviour is not clear, there is clearly a strong case for a rigorous modelling study to clarify the situation. It is interesting that, with the water/glycol mixture (Fig. 11), not only was there a monotonic increase in performance demonstrated with radius, but also the experimental values were in better agreement with the Nusselt predic-

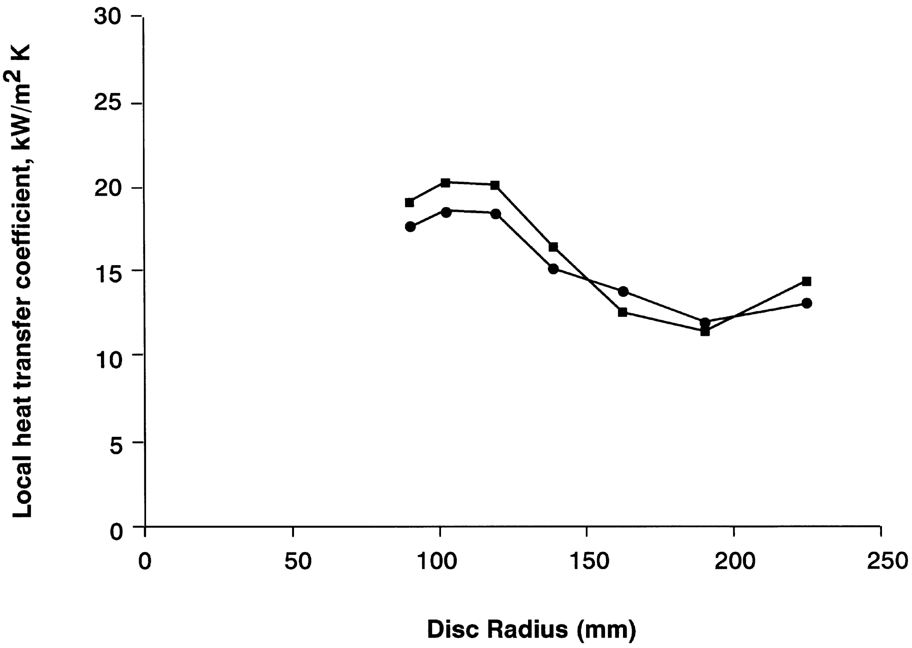

Fig. 13. Local liquid film heat transfer coefficient on smooth disc (water): 70 $cm^3 s^{-1}$, 60 s^{-1}.

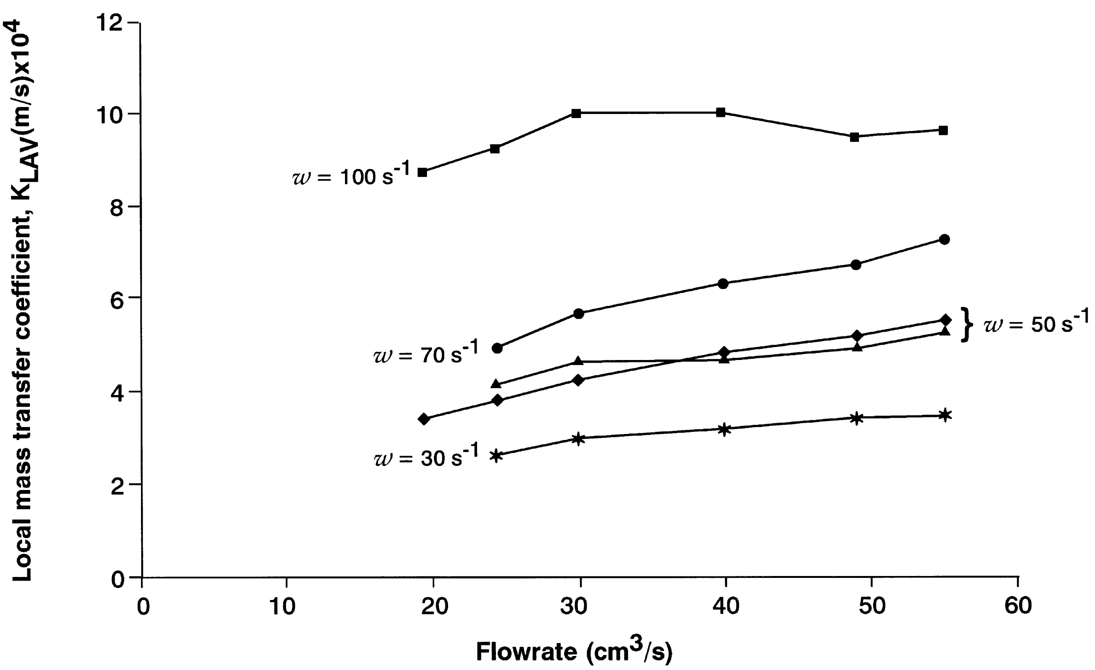

Fig. 14. Average mass transfer coefficient vs flowrate (water): flowrate = 40 $cm^3 s^{-1}$, smooth disc.

tions. Presumably the higher viscosity of this system ensured that the film behaviour conformed more closely to the assumptions implicit in the Nusselt treatment though it also had a major adverse impact on performance. Further performance enhancement from the smooth disc values can be envisaged by reconfiguring the surface to increase both the surface area and film mixing.

The mass transfer behaviour with water is shown in

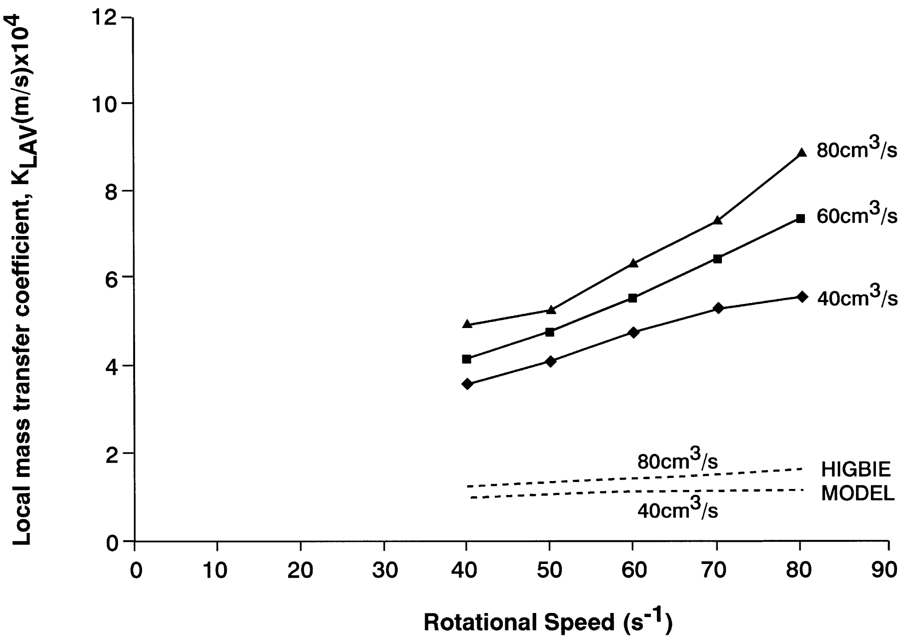

Fig. 15. Average mass transfer coefficient vs rotational speed: water, smooth disc.

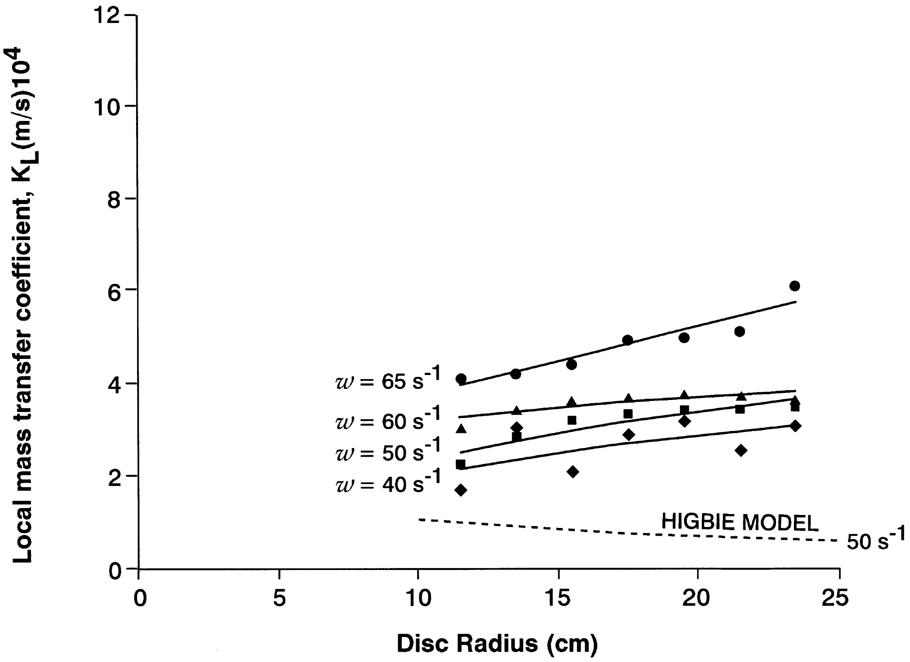

Fig. 16. Local mass transfer coefficient vs disc radius: water, flowrate = 30 $cm^3 s^{-1}$, smooth disc.

Figs 14–17, together with the predictions of the Higbie model based on the transit time of a surface element across the disc. It will be seen that the performance was surprisingly insensitive to radial position and flowrate, but was strongly influenced by rotational speed. As discussed above, performance predictions based upon the penetration theory are believed to be more relevant than a film theory interpretation. However, the Higbie model grossly underestimated the achieved values by about a factor of 5. Such a mismatch between theory and exper-

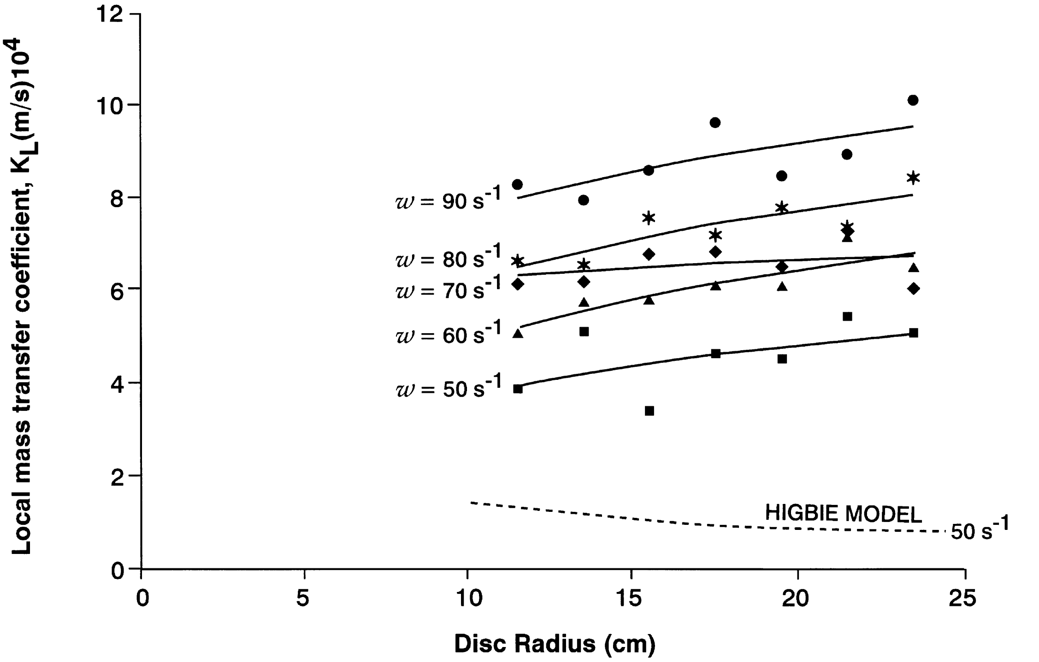

Fig. 17. Local mass transfer coefficient vs disc radius: water, flowrate = 80 $cm^3 s^{-1}$, smooth disc.

iment can only be explained by a breakdown of the model assumptions. Thus, film instability and the propagation of ripples may be expected to generate exposure times which are far less than the liquid surface residence time on the disc. This view is entirely in accord with the work of Brauner and Maron [3] but offers cold comfort to the modeller in view of the extreme complexity of the fluid dynamic environment on the disc. Further performance enhancement was achieved by modifying the disc surface characteristics and profile. Unfortunately these results cannot be quoted due to confidentiality considerations.

The high performance achieved with a rotating disc suggests that this configuration can be extensively exploited in the context of process intensification, particularly with an assembly of closely spaced discs. The progress which has already been made during the rotary heat pump development implies that a multi-functional unit is feasible, so that several process operations can be encapsulated within one compact rotating envelope. This concept is the very essence of process intensification and is being developed with a number of partners.

5. Conclusions

(i) While very high heat transfer performance can be achieved with inviscid liquid films on a smooth spinning disc, performance predictions based on a simple Nusselt analysis are not satisfactory.

(ii) Unexpectedly high heat transfer film coefficients were observed at the inner radial positions where the feed liquid was approaching the disc angular velocity.

(iii) Much lower heat transfer performance was noted with a more viscous liquid. No entrance effect was observed and there was reasonable agreement with the Nusselt predictions.

(iv) Mass transfer rates were dominated by disc speed and were only a weak function of liquid feedrate and disc radius.

(v) The Higbie model grossly underpredicted the mass transfer performance.

(vi) A generalised fluid dynamic model of the flow of liquid films over rotating surfaces is highly desirable as it would provide a firm basis for further development of this technology.

(vii) Despite the limited predictive capability of the model, the experimental data obtained in this study has confirmed the attractiveness of the spinning disc (or more generally a rotating surface of revolution) as the basis for a highly intensified reactor when dealing with rapid exothermic reactions or viscous liquids. The potential industrial applications are being progressed with a number of interested parties.

References

[1] C. Ramshaw, Opportunities for exploiting centrifugal fields, Heat Recovery Systems and CHP 13 (1993) 493–513.

[2] C. Ramshaw, Higee distillation—an example of process intensification, The Chemical Engineer, 1983, pp. 13–14.

[3] N. Brauner, D.M. Maron, Characteristics of inclined thin films, waviness and the associated mass transfer, Int. J. of Heat Mass Transfer 25(1) (1982) 99–110.

[4] W. Woods, The hydrodynamics of thin liquid films flowing over a rotating disc, Ph.D. thesis, Newcastle University, 1995.

[5] C. Ramshaw, T.L. Winnington, An intensified absorption heat pump, Proc. Inst. Refrigeration 85 (1988) 26–31.

[6] W. Nusselt, Die Oberflächenkondensation des Wasserdampfes, Z. Ver. deut. Ing. 60 (1916) 541.

[7] H.S. Carslaw, J.C. Jaeger, Conduction of Heat in Solids, 2nd ed., OUP, 1959.

[8] W.G. Whitman, The two film theory of absorption, Chem. and Met. Eng. 29 (1923) 147.

[9] R. Higbie, The rate of absorption of pure gas into a still liquid during short periods of exposure, Trans. A.I.Ch.E. 31 (1935) 365.